

# We are IntechOpen, the world's leading publisher of Open Access books Built by scientists, for scientists

6,900

Open access books available

186,000

International authors and editors

200M

Downloads

Our authors are among the

154

Countries delivered to

TOP 1%

most cited scientists

12.2%

Contributors from top 500 universities



WEB OF SCIENCE™

Selection of our books indexed in the Book Citation Index  
in Web of Science™ Core Collection (BKCI)

Interested in publishing with us?  
Contact [book.department@intechopen.com](mailto:book.department@intechopen.com)

Numbers displayed above are based on latest data collected.  
For more information visit [www.intechopen.com](http://www.intechopen.com)



# Chemical Signal Guided Autonomous Underwater Vehicle

Shuo Pang  
Embry-Riddle Aeronautical University  
USA

## 1. Introduction

Olfaction is a long distance sense, which is widely used by animals for foraging or reproductive activities (Dusenbery, 1992; Vickers, 2000; Zimmer & Butman, 2000): homing by Pacific salmon (Hassler & Scholz, 1983), homing by green sea turtles (Lohmann, 1992), foraging by Antarctic procellariiform seabirds (Nevitt, 2000), foraging by lobsters (Basil, 1994), foraging by blue crabs (Wiesburg & Zimmer-Faust, 1994), mating and foraging by insects (Cardé & Mafra-Neto, 1997). Olfaction plays a significant role in natural life of most animals. For some animals, olfactory cues are far more effective than visual or auditory cues in search for objects such as foods and nests (Bell & Tobin, 1982). Although odor sensing is far simpler than vision or hearing, navigation in a chemical diffusion field is still not well understood (Lytridis et al., 2006). Therefore, this powerful primary sense has rarely been used inside the robotics community.

For many military and civilian applications in turbulent fluid flow environment, it would be useful to detect and track a chemical plume to its source. Chemical Plume Tracing (CPT) program, which is sponsored by US Office of Naval Research (ONR), seeks to learn how animals successfully accomplish similar tasks, and to develop algorithms for plume tracing using Autonomous Underwater Vehicles (AUVs). AUVs capable of such chemical plume tracing feats would be of great significance for many applications, e.g., the detection of chemical leaks, locating unexploded ordnance, and locating biologically interesting phenomenon such as thermal vents.

This chapter describes the development and field test of a chemical signal guided REMUS AUV system to find a chemical plume, trace the chemical plume to its source, declare reliably the source location, and map the plume source area after source declaration. The basic idea of the chemical signal guided AUV system is illustrated in Fig. 1. An AUV is constrained to maneuver within a region referred to as the OpArea. Within the OpArea the AUV should search for a specified chemical, for which a binary sensor is available. The mission starts with the AUV searching the OpArea for the chemical plume. A binary sensor outputs 1.0 if the chemical concentration is above threshold or 0.0 if the chemical concentration is below threshold. If above threshold chemical is detected, the AUV should trace the chemical plume to its source and accurately declare the source location. Following the source declaration, additional AUV maneuvers might be desired to acquire additional data, possibly using auxiliary sensors. The plume depicted in Fig. 1 is greatly simplified.

Source: Underwater Vehicles, Book edited by: Alexander V. Inzartsev,  
ISBN 978-953-7619-49-7, pp. 582, December 2008, I-Tech, Vienna, Austria

Realistic plumes may meander, are intermittent or patchy distributions of chemical, and do not have a uniformly increasing width as a function of the distance from the chemical source.

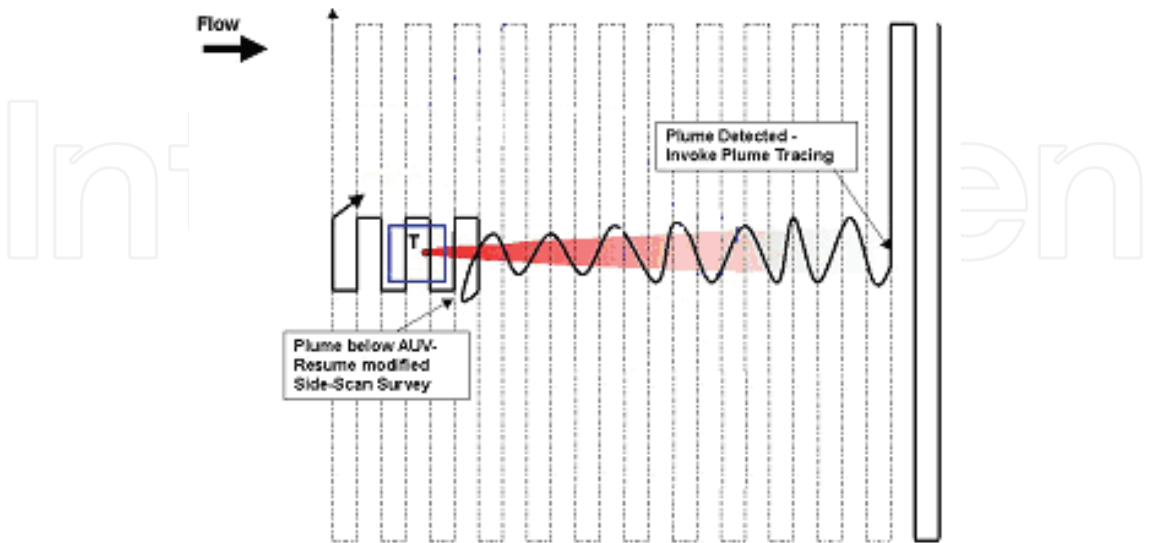


Fig. 1. A prototype CPT mission with post-declaration maneuvering. The depicted plume is a rendition that does not attempt to include intermittency or meander.

A typical vehicle hardware, control, guidance, mapping, and planning architecture for chemical plume tracing are shown in Fig. 2. The figure shows that the assumed inputs to the on-line mapping system are sensed concentration  $c(p_v(t_i))$ , vehicle location  $p_v(t_i)$ , and flow velocity  $u(t_i) = (u_x(p_v(t_i)); u_y(p_v(t_i)))$  at time  $t_i$ . The online planner would optimize a desired vehicle trajectory based the online map. The guidance system outputs heading, speed and depth commands to the controller to achieve the planner's desired trajectory without violating the heading and velocity constraints.

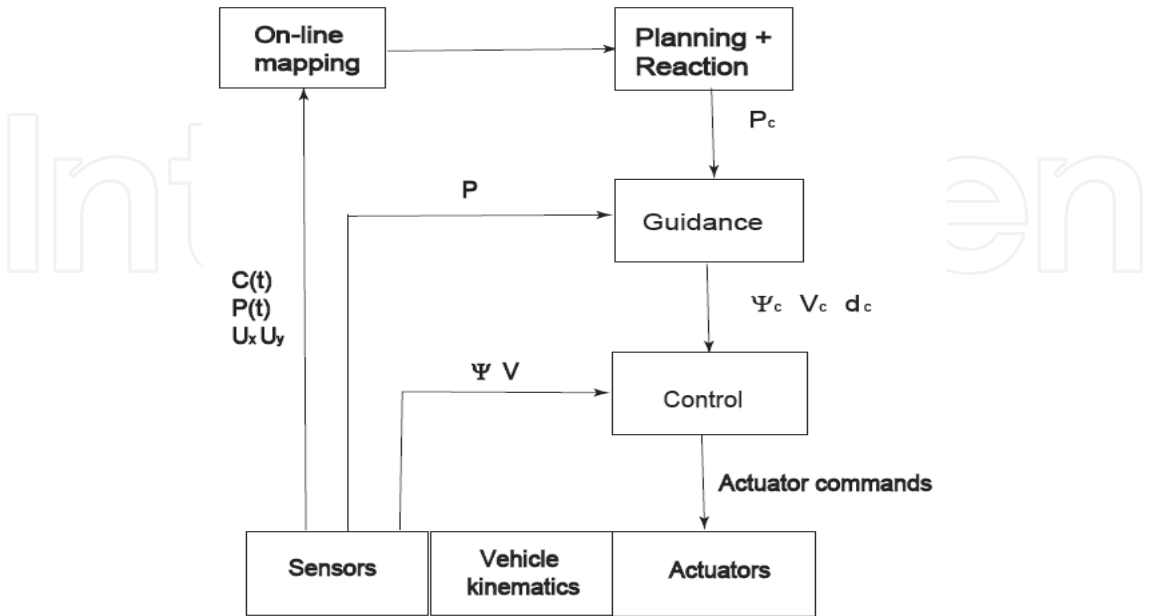


Fig. 2. AUV based Chemical Plume Tracing Architecture.

## 2. Background

Chemical signal guided search is complicated by the nature of fluid flow and the resulting odor plume characteristics. An initial approach to designing an AUV chemical plume-tracing strategy might attempt to calculate a concentration gradient. Gradient following based plume navigation algorithms have been proposed for a few biological entities that operate in low Reynolds number environments (Berg, 1990); however, gradient based algorithms are not feasible in environments with medium to high Reynolds numbers (Elkinton et al., 1984; Jones, 1983; Murlis et al., 1992). At low Reynolds numbers, the evolution of the chemical distribution in the flow is dominated by molecular diffusion resulting in a chemical concentration field that is reasonably well-defined by a continuous function with a peak near the source. At medium and high Reynolds numbers, the evolution of the chemical distribution in the flow is turbulence dominated (Shraiman & Siggia, 2000). The flow contains eddying motions of a wide range of sizes that produce a patchy and intermittent distribution of the above threshold chemical (Jones, 1983). For an image of the plume, the gradient is time-varying, steep, and frequently in the wrong direction. Even so, such plume images are not available to the AUV. Due to the rate of spatial and temporal variations in the flow and plume relative to the maneuvering limitations of existing AUV, gradient computation and following is not practical.

If a dense array of sensors were distributed over an area through which a turbulent flow was advecting chemical and the output of each sensor were averaged for a suitably long time (i.e., several minutes), then this average chemical distribution would be Gaussian (Sutton, 1947; Sutton 1953); however, the required dense spatial sampling and long time-averaging makes such an approach inefficient in a turbulence dominated environment (Naeem et al., 2007). It is known that the instantaneous chemical distribution will be distinct from the time-averaged plume (Jones, 1983; Murlis et al., 1992). The major differences include: the time-averaged plume is smooth and unimodal while the instantaneous plume is discontinuous and multi-modal; the time-averaged plume is time invariant (assuming ergodicity) while the instantaneous plume is time varying; instantaneous concentrations well-above the time-averaged concentration will be detected much more often than predicted by the Gaussian plume model. Such time-averaged plumes are useful for long-term exposure studies, but are not useful for studies of responses to instantaneously sensed chemical (Murlis et al., 1992). One of the reasons that olfaction is a useful long distance sense is the fact that instantaneous concentrations well above the time-average are available at significant distances from the source (Grasso, 2001). Turbulent diffusion results in filaments of high concentration chemical at significant distances from the source, but also results in high intermittency (Jones, 1983; Murlis et al., 1992; Mylne, 1992). Intermittency increases with down flow distance both due to the meander of the instantaneous plume caused by spatial and temporal variations in the flow and due to the increasing spread with distance of the filaments composing the instantaneous plume. High intermittency and large search areas motivate the need to acquire as much information as is possible from each chemical detection event.

The challenge using chemical signals on AUV is to design effective algorithms to trace the chemical plume and determine the chemical source location even though the chemical source concentration is not known, the advection distance of the detected chemical is unknown, and the flow varies with both location and time.

Various studies have developed biomimetic robotic plume tracing algorithms based on olfactory sensing. The most commonly used olfactory-based navigation algorithms is "chemotaxis", which was introduced by Berg and Brown (Berg & Brown, 1972; Berg, 1993). This strategy is based on the detection of a concentration difference between two chemical sensors and a steering mechanism toward the direction of higher concentration with a constant moving speed. Chemotaxis-based navigational strategies yield smooth movement trajectories in the environment that the concentration is high enough to ensure its difference measured at two nearby locations is larger than typical fluctuations. Belanger and Willis (Belanger & Willis 1998) presented plume tracing strategies inspired by moth behavior and analyze the performance in a "wind tunnel-type" computer simulation. The main goal of that study was to improve the understanding of moth interaction with an odor stimulus in a wind tunnel. Grasso et al. (Grasso et al. 1996; Grasso, 2001; Grasso, et al., 2000) evaluate biometric strategies and challenge theoretical assumptions of the strategies by implementing biometric strategies on their robot lobster. Li et al. (Li et al., 2001; Li et al., 2006) develop, optimize, and evaluate a counter-turning strategy originally inspired by moth behavior. Vergassola et al. (Vergassola et al., 2007; Martinez 2007) proposed a search algorithm, "infotaxis", based on information and coding theory. For infotaxis, information plays a role similar to concentration in chemotaxis. The infotaxis strategy locally maximizes the expected rate of information gain. Its efficiency was demonstrated using a computational model of odor plume propagation and experimental data on mixing flows. Infotactic trajectories feature zigzagging and casting paths similar to those observed in the flight of moths. Spears et al. (Spears et al., 2005; Zarzhitsky et al., 2004) developed a physics-based distributed chemical plume tracing algorithm. The algorithm uses a network of mobile sensing agents that sense the ambient fluid velocity and chemical concentration, and calculate derivatives based on formal principles from the field of fluid mechanics.

The fundamental aspects of these research efforts are sensing the chemical, sensing or estimating the fluid velocity, and generating a sequence of searcher speed and heading commands such that the motion is likely to locate the odor source. Typical maneuvers include: sprinting upflow upon detection, moving crosswind when not detecting, and manipulating the relative orientation of a multiple sensor array either to follow an estimated plume edge or to maintain the maximum mean reading near the central sensor. In each of these articles, the algorithms for generating speed and heading commands use only instantaneous (or filtered) sensor readings.

This chapter extends plume tracing research by presenting a complete strategy for finding a plume, tracing the plume to its source, and maneuvering to accurately declare the source location; and, by presenting results from successful, large-scale, in-water tests of this strategy. The assumptions made herein relative to the chemical and flow are that the chemical is a neutrally buoyant and passive scalar being advected by a turbulent flow. The AUV is capable of sensing position, concentration, and flow velocity. The concentration sensor is used as a binary detector (above or below threshold). We solve the plume-tracing problem in two dimensions. A main motivation for implementing the algorithms in two dimensions is the computational simplification achieved; however, neutral buoyancy of the chemical or stratification of the flow (Stacey, 2000) will often result in a plume of limited vertical extent, which may be approximated as two-dimensional.



### 3. Behavior based planning method

Chemical signal guided search is a complicated problem. One way to reduce the complexity is to break down the planning problem into a set of simpler subproblems each solvable by simpler actions with an appropriate method to switch between actions. This divide-and-conquer strategy is effective in many planning applications that deal with complex systems. These simpler actions are called behaviors. A behavior is a mapping of sensor inputs to a pattern of motor actions, that accomplishes a single goal within a restricted context. A behavior-based planning (BBP) strategy is an efficient means to navigate an autonomous system in an uncertain environment. To use a set of behaviors to achieve a task a mechanism for coordinating the behaviors is also required.

In the late 1970's and early 1980's, Arbib began to investigate models of animal intelligence from the biological and cognitive sciences point-of-view to gain alternative insight into the design of advanced robotic capabilities (Arbib, 1981). At nearly the same time, Braitenberg studied methods by which machine intelligence could be evolved by using sensor-motor pairs to design vehicle systems (Braitenberg, 1984). Later, a new generation of AI researchers began exploring the biological sciences in search of new organizing principles and methods of obtaining intelligence. This research resulted in the reactive behavior-based approaches. Brooks' subsumption architecture is the most influential of the purely reactive paradigms. Its basic idea is to describe a complex task by several behaviors, each with simple features (Brooks, 1986). Design of a behavior-based planner includes two significant steps. First, the designer must formulate each reactive behavior quantitatively and implement the behavior as an algorithm. Second, the designer must define and implement a methodology for coordinating the possibly conflicting commands from the different behaviors to achieve good mission performance.

Various coordination approaches have been proposed. For example, each behavior can output a command and a priority. Traditional binary logic can be used to select and output the command with the highest priority. An alternative coordination approach is to use artificial potential fields (Arkin & Murphy 1990). A drawback to either approach is that formulating and coordinating the reactive behaviors requires significant pre-mission simulation and testing. These are ad-hoc processes and may need to be re-addressed each time new behaviors are added or existing behaviors are changed. In some applications, these tuning parameters depend heavily on environmental conditions. Another alternative that has been suggested is to train an artificial neural network (ANN) to perform the behavior coordination (Li et al., 1997). However, this approach would require some mechanism for determining "correct" coordination decisions for each training scenario and would provide no guarantee that all coordination situations are properly trained (Berns et al., 1991). Fuzzy control methods can improve the performance of reactive behavior coordination (Li et al. 1997) by providing a formalism for automatically interpolating between alternative behaviors. Although similar in overall structure, fuzzy control differs from classic feedback control. In fuzzy control, the controller has the same function inputs and outputs as in the feedback control, but internally the control values are computed using techniques from fuzzy logic. Fuzzy controller takes fuzzy state variables, by applying sets of fuzzy rules, produces a set of fuzzy control values. These fuzzy control values are not precise numbers, but rather represent a range of possible values with different weights. Eventually, a decision is made based on the fuzzy control values.

Behavior based design methodologies are bottom-up approaches to the design of an intelligent system. Observed behaviors with simple features are analyzed and synthesized independently. By using these design methodologies, we break down the complicated plume tracking problem into five behaviors. Later in this chapter, we will describe the behaviors and coordination mechanism that were used to solve the problem of chemical plume tracing strategy for an AUV in details. The behaviors were inspired by behaviors observed in biological entities.

#### 4. AUV guidance system

A typical AUV chemical plume tracing system includes an adaptive mission planner (AMP) that rapidly responds to the sensor inputs to generate a trajectory for the AUV to trace the plume. Because the AUV has velocity ( $<2$  m/sec) and heading rate ( $<10$  degree/sec) constraints and the vehicle navigation system has navigation fixes (The vehicle is performing dead-reckoning based on acoustic Doppler data with periodic navigation updates based on data from a long baseline acoustic buoy transponder system. The position updates to the dead-reckoned position based on the LBL data are referred to as navigation fixes), a guidance system is necessary for the AUV to generate heading and speed commands within the constraints to achieve the trajectory desired by the AMP. "Guidance is the action of determining the course, attitude and speed of the vehicle, relative to some reference frame, to be followed by the vehicle" (Fossen, 1994). For the chemical signal guided AUV, the guidance system combined with the AMP decides the best trajectory to be followed by the AUV based on the chemical information and vehicle capability. Although many guidance systems exist for use on the land and air vehicles, there are few, if any systems designed for AUVs (Naeem et al., 2003).

The AUV guidance system is divided into four guidance modes: Go To Point mode, Follow Line mode, Go To Point with Heading mode, and Cage mode. The Go To Point mode is used to drive the AUV from its present location to a destination, without regard to the heading at the destination location. The Follow Line mode is used to track a straight line. The Go To Point with Heading mode is to drive the AUV from a start position and orientation angle to a destination position and orientation angle with the constraint that desired trajectory cannot violate a prespecified minimum turning circle. The Cage mode prevents the vehicle from leaving the operating area or return the vehicle to the operating area if it has left the operating area. To ensure the outputs of the guidance system do not violate the heading rate constraint, the heading commands are filtered before they are sent to the vehicle control unit. In any of these modes, the guidance function will output depth/altitude and earth relative velocity (geographic heading and speed) commands that are within the velocity and heading rate constraints of the AUV. For accurate implementation of the desired trajectory, the guidance system should compensate these commands for the flow vector to produce water relative speed  $u_c$  and ground relative heading commands  $\Psi_g^t$ :

$$V_f = V_g - F_g \quad (1)$$

$$\Psi_g^t = a \tan 2[(v_f, u_f)^t] \quad (2)$$

$$V_c = \|V_f\| \quad (3)$$

where  $V_f = (u_f, v_f, w_f)$  is the water relative AUV velocity,  $V_g$  is the ground relative AUV velocity, and  $F_g$  is the ground relative flow vector. A superscript indicates a coordinate frame: "t" for geodetic tangent frame or "b" for body frame. The components of vector  $V_g^t$  are  $(u_f, v_f, w_f)^t$ .

#### 4.1 Go to point

This mode is used to drive the vehicle from its present location to a destination, without regard to the heading at the destination location, e.g., initialize the plume search from a desired point, go to next search region after the vehicle finish searching in the current region, or return to home location after the vehicle finish its mission.

When the guidance system is in Go To Point mode, the output of the system is the geographic heading command

$$\Psi_c = \arctan\left(\frac{y(t) - y_d}{x(t) - x_d}\right) \quad (4)$$

and a constant speed command

$$V_c(t) = v \quad (5)$$

where  $(x(t), y(t))$  is the current vehicle position,  $(x_d, y_d)$  is the destination location, and  $v$  is a predefined constant speed. Note, the heading angle  $\Psi_c \in [0, 360]$  is defined in degrees and goes clockwise. When the vehicle is within a radius  $R$  of the destination location,

$$\sqrt{(x(t) - x_d)^2 + (y(t) - y_d)^2} < R \quad (6)$$

where  $R$  is a predefine value, it is considered to have arrived at the destination location and the guidance system will exit from the Go To Point mode.

This mode is the most robust mode in our guidance system. Because unlike the other modes in our guidance system, the vehicle does not try to follow a precalculated trajectory, instead it calculates its trajectory based on the real time vehicle location information. Therefore, when we have navigation fixes and curvature constrains during the vehicle traveling, the vehicle trajectory is modified accordingly.

#### 4.2 Follow line

Sometimes the vehicle needs to track a straight line, e.g. the vehicle doing a lawn mower search, or the vehicle doing a side scan maneuver after it declares the source location. Given two locations  $(x_s, y_s)$  and  $(x_d, y_d)$  in the OpArea, we can get a line segment  $L_{sd}$  which starts from point  $(x_s, y_s)$  and ends at point  $(x_d, y_d)$ . The Follow Line mode will generate a set of heading and speed commands which will make the vehicle follow the line  $L_{sd}$ . The first step to achieve follow line mode is to drive the vehicle to approach the start point  $(x_s, y_s)$  while ensuring that the vehicle heading  $\Psi$  upon arrival at the start of the line is about the same as the line orientation angle,

$$\alpha_{sd} = \arctan\left(\frac{y_d - y_s}{x_d - x_s}\right). \quad (7)$$



Here we cannot use Go To Point mode, because it cannot satisfy the heading condition. So we design a new mode Go To Point with Heading to achieve this work. This mode will be discussed later. When the vehicle is within radius  $R$  of the start point and within heading angle  $\theta$  of  $\alpha_{sd}$ , the vehicle will begin to follow the line. The corresponding heading command is

$$\psi_c(t) = \begin{cases} \alpha_{sd} + K \times d & d < d_1 \\ \alpha_{sd} + \text{sign}(d) \times 45 & d \geq d_1 \end{cases} \quad (8)$$

where  $d$  is the signed distance between the vehicle current position  $P(t) = (x(t), y(t))$  and the line  $L_{sd}$ ,  $K$  is a predefined gain,  $d_1 = 45/K$ , and the sign function is defined

$$\text{sign}(x) = \begin{cases} 1 & x \geq 0 \\ -1 & x < 0 \end{cases} \quad (9)$$

Note, the distance  $d$  is positive when the vehicle is on the left side of the line  $L_{sd}$  (when looking from the start point  $(x_s, y_s)$  to the destination point  $(x_d, y_d)$ ), and negative when the vehicle is on the right side of the line.

The exit condition for this mode is different from Go To Point mode. In Go To Point mode, we exit the mode when the vehicle is within a radius  $R$  of the destination location. Here in the Follow Line mode, we can still use this condition. However, since there are some navigation fixes during the vehicle traveling, the vehicle trajectory is not continuous; it contains some jumps in the trajectory. These jumps may happen near the destination point, therefore the vehicle may jump over the destination point without being within radius  $R$ , and it will continue following the line until it hits the edge of the OpArea. To prevent this, we need to add one additional exit condition for this mode. When the vehicle pass the destination point in the direction of the line for more than  $R_L$  meters we suppose that the vehicle has finished the follow line mode and it exits from this mode. That is, if

$$V \bullet h > R_L \quad (10)$$

where vector  $V = [x - x_d, y - y_d]$ , and  $h = [\cos(\alpha_{sd}); \sin(\alpha_{sd})]$  is a unit vector in the direction of the line, then we exit from the follow line mode.

Fig. 3 shows an example of follow line mode. The vehicle is start from position  $P_1(x_1, y_1)$ . Go To Point with Heading function drives the vehicle to the position  $P_2(x_s, y_s)$ , which is within a radius  $R$  of the start position  $(x_s, y_s)$  with heading error less than 15 degrees. Then, the vehicle will follow the line based on the heading command defined in equation (8) until either condition (6) or condition (10) is satisfied.

### 4.3 Go to point with heading

The goal of this mode is to drive the AUV from a start position and orientation angle to a destination position and orientation angle with the constraint that desired trajectory cannot violate a prespecified minimum turning circle. This guidance mode is significantly more complicated than it first appears. It was proved by Dubins (Dubins, 1957) that this trajectory consists of exactly three path segments. It is either a sequence of CCC or CSC, where C (circle) is an arc of minimal turning radius  $R_m$  and S (straight line) is a line segment. In our application, we only use the CSC trajectory. Even though the CSC trajectory sometimes is not the shortest path, it is easy to generate this trajectory, thereby saving computation resources.

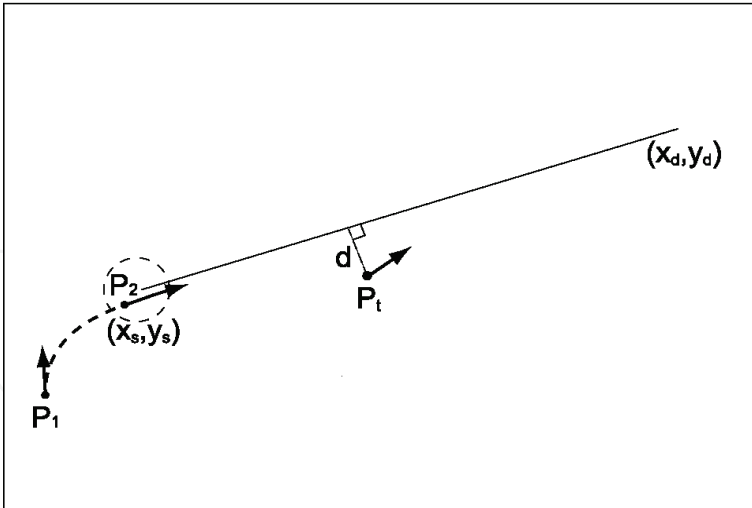


Fig. 3. Definition of variables for the Follow Line mode.

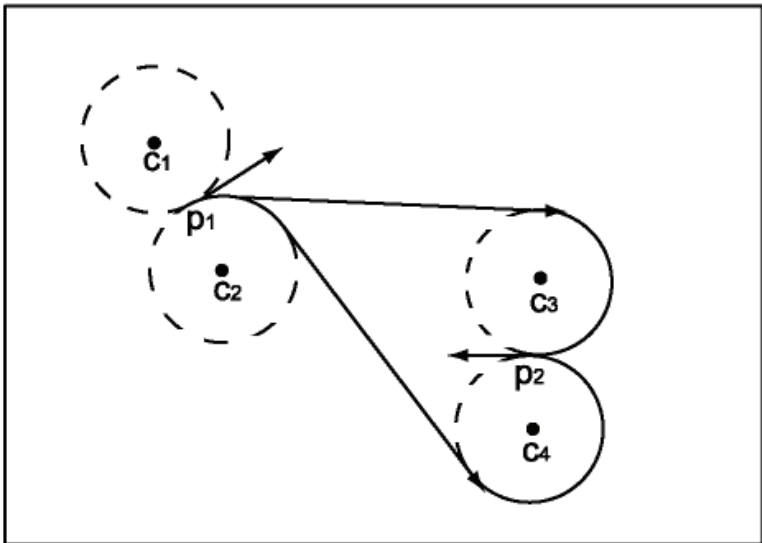


Fig. 4. Depiction of the Go to Point With Heading mode.

Fig. 4 shows an example of Go to Point with Heading mode. The AUV starts from position  $p_1$  with orientation angle  $\theta_1$  and should go to position  $p_2$  with orientation angle  $\theta_2$ . Here we use two unit vectors  $V_1$  and  $V_2$  to represent the start and destination positions and orientation angles. First, we generate four circles  $C_1, C_2, C_3, C_4$ , whose radii are the minimal allowed turning radius  $R_m$ . The first two circles  $C_1, C_2$  are tangent to  $V_1$  at  $p_1$ ,  $C_3, C_4$ , are tangent to  $V_2$  at  $p_2$ . Note that arcs  $C_1, C_4$  are counterclockwise and  $C_2, C_3$  are clockwise. Second, we generate four line segments  $L_{ij}$ , where  $i=1,2$  and  $j=3,4$  (only showing two lines in Fig. 4). Line  $L_{ij}$  connects  $C_i$  to  $C_j$  in a continuous fashion. Now, we have four possible candidate paths, namely,  $C_1L_{13}C_3; C_1L_{14}C_4; C_2L_{23}C_3; C_2L_{24}C_4$ . Third, we calculate the length for each of the four candidate paths and select the shortest path as the trajectory for the AUV.

4.4 Cage

The Cage mode has two responsibilities related to the safety of the AUV. First, it should prevent the AUV from leaving the operating area or return the AUV to the operating area if it has left the operating area. Second, if the AUV is more than 30 m outside the operating

envelope, then the Cage mode must abort the mission. Aborting the mission in the latter case is straightforward.

When the AUV is outside the OpArea or is near (within 5 m) an edge, we find the outward unit normal  $N=[N_e, N_n]$  and the distance  $\delta$  to the nearest edge. If the AUV is inside the OpArea (i.e.,  $0 < \delta < 5$ ), then the commanded heading that results from the guidance system is modified to remove a portion of its outward component:

$$V = [\cos(\psi_c), \sin(\psi_c)] \quad (11)$$

$$T = V - (1-\delta/5)(V^T N)N \quad (12)$$

$$\psi_c = \text{atan2}(T_1, T_2) \quad (13)$$

where “atan2” is the four quadrant arc tangent function. Therefore, when inside the OpArea, the AUV should not drive itself out of the OpArea; however, a navigation fix could instantaneously change the computed AUV position to be outside of the OpArea. If the AUV is outside the OpArea, then the heading command is  $\psi_c = \text{atan2}(-N_e, -N_n)$ .

## 5. Behavior based chemical plume tracing

Fig. 5 displays the behaviors and switching logic used to implement CPT algorithms using BBP. In Fig. 5,  $S$  and  $d$  are Boolean variables. The symbols  $S$  and  $\bar{S}$  indicate that the source location has or has not been declared, respectively. The symbol  $d$  indicates that chemical has been detected. The symbol  $\bar{d}$  indicates that the behavior completed without detecting chemical. Prior to source declaration, whenever chemical is detected, the Track-In behavior

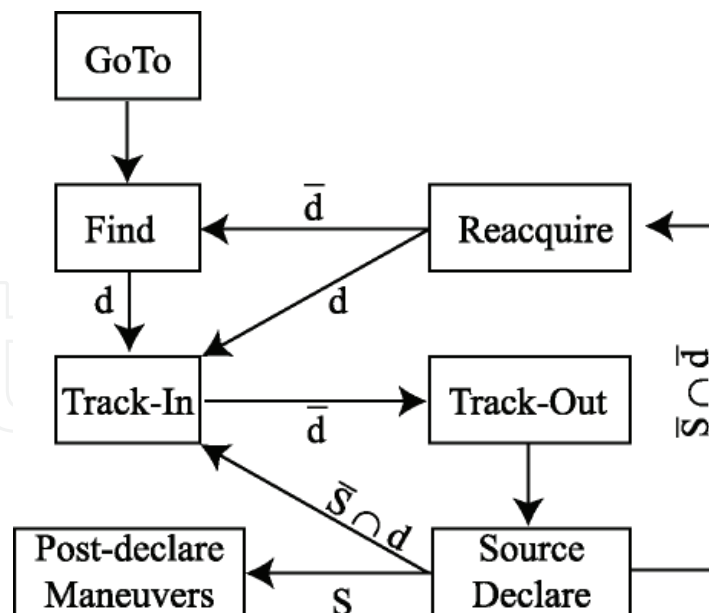


Fig. 5. Behavior Switching Diagram. The symbol  $d$  denotes a behavior switch that occurs when chemical is detected. The symbol  $\bar{d}$  denotes a behavior switch that occurs when chemical is not detected prior to the end of the behavior.  $S$  indicates that the source location has been declared.  $\bar{S}$  indicates that the source location has not been declared.

is triggered. Due to the intermittency caused by the turbulent flow, an instantaneous chemical reading below the detection threshold does not necessarily imply that the AUV is “out of the plume.” Therefore, the sequence of behaviors Track-Out, Reacquire, Find is instantiated as the time since the last detection increases. The specific aspects of each behavior and the logic for switching between the behaviors are described in later. The planner is implemented on a PC104 computer that will be referred to as the Adaptive Mission Planner (AMP).

### 5.1 Go-To behavior

The Go-To behavior is used to drive the vehicle to a desired location. This is used for example at the start of a mission to maneuver the vehicle to a desired starting location. The Go-To behavior directly executes the Go-To guidance command.

### 5.2 Find behavior

Since there is no prior information about the location of the source, the AUV may be required to search the entire OpArea. Since the odor plume will be downflow from the source, the search is designed to start at the most downflow corner of the OpArea. From this starting location, the AUV should proceed across the flow until it either reaches a boundary of the OpArea or detects chemical. Although the largest component of the commanded velocity is across the flow, there must also be a component either up or down the flow so that the AUV will explore new locations in the OpArea. If chemical is detected, then the behavior switches to Track-In. If the AUV meets the boundary without detecting chemical, then the reaction is described below.

When the AUV arrives at a boundary, four candidate directions are computed as:  $\psi_f \pm 90 \pm 20$ , where  $\psi_f$  is the flow direction in degrees. Of these four candidate directions, the behavior selects the direction that maintains the same sign of the velocity along the boundary and reverses the sign of the velocity perpendicular to the boundary. When none of the four candidates satisfies this condition, then the motion is continued parallel to the boundary until the condition is achieved or another boundary is met. At such a corner, two directions of motion must be changed, and the solution can always be found. When the flow is parallel to a boundary, then this Find strategy results in a billiard ball type of reflection at the OpArea boundary.

### 5.3 Track-In behavior

Studies described in (Li et al., 2001) show that immediately following a chemical detection, good plume tracking performance is attained by driving at an angle  $\beta \in [20, 70]$  degree offset relative to upflow. When driving at a nonzero angle  $\beta$  offset relative to upflow and contact with the plume is ultimately lost, the AUV can predict which side of the plume it exited from and perform a counterturn to reacquire the plume. Such counterturning strategies are exhibited in several biological entities. The Track-in behavior implements an engineered version of such a strategy.

Pseudo-code for the Track-In behavior is contained in Table 1. The AMP will stay in Track-In behavior as long as there has been an above threshold concentration sensed in the last  $\lambda$  seconds. While chemical is being detected, AMP adjusts the commanded heading  $\psi_c$  to be offset by  $LHS \cdot \beta$  relative to the upflow direction  $\psi_u = \psi_f + 180$ . In this expression  $\beta$  is a

constant and LHS is a variable that switches based on the relative directions of the AUV and flow. LHS is 1 if we expect the AUV to drive out of the plume from the left side (when looking upflow) of the plume. Otherwise, LHS is -1. Each time chemical is detected, the current AUV position is saved; therefore, when Track-In exits, the last detection point is available and saved in a list named `lost_pnts`.

```
Behavior::track_in( )
{
    v=vc;
    if(odor conc. >= threshold)
    { // Stay in track in
         $\psi_c = \psi_f + 180 + LHS*\beta$ ;
        if ( $\psi_v - \psi_f < 180$ )
            LHS =1;
        else
            LHS =-1;
        Tlast = t;
        last_detection_point = position;
    }
    else if((t - Tlast) >  $\lambda$ )
    { // Go to track out
        // save last detection point
        lost_pnts[i]=last_detection_point;
        i++;
        return track_out;
    }
    return track_in;
}
```

Table 1. Pseudo Code for Track-In Behavior

As long as the AUV is detecting chemical at least every  $\lambda$  seconds, it will make up flow progress. The actual AUV trajectory will include small angle, counter-turning oscillations relative to the upflow direction. If the AUV fails to detect chemical for  $\lambda$  seconds, then AMP saves the last detection point (at most 6 points are saved) and switches to Track-Out.

5.4 Track-Out behavior

Pseudo-code for the Track-Out behavior is contained in Table 2. When the AMP switches to Track-Out, it has detected chemical slightly more than  $\lambda$  seconds previously; in addition, there will be at least one point on the list of last detection points. Normally, the most recent detection point will be the last one on the list; however, since other behaviors manipulate the list, this is not guaranteed. Also, the variable LHS indicates on which side of the plume the AUV was located when contact with the plume was lost.

The Track-Out behavior attempts both to make progress towards the source (upflow) and to quickly reacquire contact with the plume. To accomplish these two objectives, AMP commands the AUV to go to a point that is  $L_u$  meters upflow and  $L_c$  meters across the flow from the most upflow point on the list of last detection points. The crossflow direction is



selected so that, if chemical is not detected, the AUV is expected to end up on the opposite side of the plume, since crossing the plume increases the likelihood of detecting chemical. Track-Out ends either when chemical is detected or the AUV arrives at the commanded location. In either case the BBP checks whether it can declare a source location prior to determining the next maneuver. If the source is declared, then post-declaration maneuvering begins. If chemical is detected and the source location cannot be declared, then the behavior switches to Track-In. In this case, the AUV is at a location further up the plume than the previous most upflow detection point. If the AUV arrives at the commanded point without detecting and the source location cannot be declared, then the behavior switches to Reacquire.

Table 2. Pseudo Code for Track-Out Behavior.  $F$  is a unit vector in the direction of the flow.  $F_p$  is rotated positively by 90 degree relative to  $F$  in the horizontal plane.  $R$ ,  $L_u$ , and  $L_c$  are positive constants.

<pre>Behavior::reacquire( ) {   if(odor conc. &lt; threshold){     pnt= find_upflow_last_pnt();     if(n &lt; N_re){       center_pnt=pnt -         10(N_re-1-n)/(N_re-1)*F;       if(bow_tie(center_pnt)== done)         n++;     }     else{       n = 0;       remove_pnt_from_list(pnt);       if(last_pnt_list_is_empty())         return find;     }     return reacquire;   }   else{     n = 0;     return track_in;   } }</pre>
--

Table 3. Pseudo Code for Reacquire Behavior

5.5 Reacquire behavior

Pseudo-code for the Reacquire behavior is contained in Table 3. When the AMP switches to Reacquire, it has not detected chemical for several seconds; however, there will be at least one point on the list of last detection points. Also, the variable LHS indicates the side of the plume on which the AUV was when it lost contact with the plume. To switch to the Reacquire behavior, the Track out behavior must have completed without detecting chemical. Therefore, several scenarios could have occurred:

- The AUV could be upflow from the source.
- The AUV could have crossed the (intermittent) plume without detecting chemical.
- If the LHS variable was incorrect, then the AUV would have moved further across the flow in the direction away from the plume.

In any of these cases, the AUV should next maneuver relative to the most upflow detection point. This Reacquire maneuver must be achievable by the AUV and useful in any of the three circumstances.

The maneuver that we designed, referred to as a Bowtie, is depicted in Fig. 6. The Bowtie maneuver first tracks a line that starts on the side of the plume on which we estimate that the AUV is located. This line is angled -15 degrees relative to upflow. The upflow 15 degree angle is small enough so that the transition to Track-In is smooth, if chemical is detected. If that line completes without a detection, then the AUV transitions to the start of a second line that passes through the same center point, but has an angle of 15 degrees relative to upflow. In Fig. 6, the narrow lines indicate distances while the wide lines show the nominal AUV trajectory. If the Bowtie completes without a detection, then the last line would be followed by a clockwise turn toward downflow, which would have a radius of at least 5.0 m.

Therefore, this maneuver explores at least 13 m on each side of its center in the direction perpendicular to the flow.

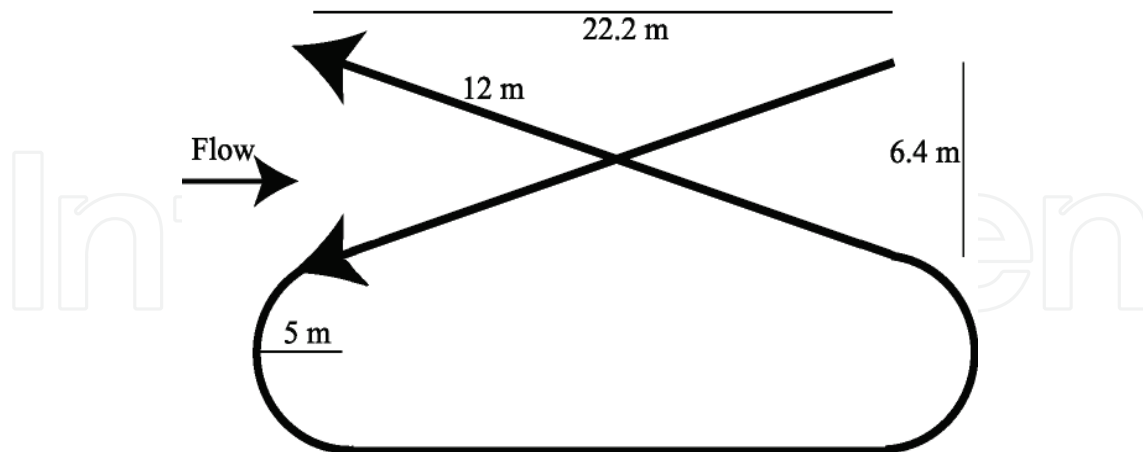


Fig. 6. Illustration of the BOWTIE maneuver used during the Reacquire maneuver. The image is not to scale.

The Reacquire behavior will perform at most  $N_{re}$  ( $>1$ ) repetitions of the Bowtie in the vicinity of a single point on the lost point list. The first Bowtie is centered 10 m upflow from the most upflow point on the list of last detection points. The last Bowtie is centered on the most upflow point on the list of last detection points. The remaining ( $N_{re}-2$ ) Bowtie centers are equally spaced between the first and last centers.

If this sequence of  $N_{re}$  Bowties completes without chemical detection, then the behavior removes the most upflow point from the list of last detection points. It then repeats the behavior at the most upflow point on the remaining list. This process repeats until a detection occurs or the list becomes empty. A detection at any time switches the behavior to Track-In. If the list becomes empty, then the AUV reverts to the Find behavior.

If the AUV started the Reacquire behavior upflow from the source, the shape of the Bowtie repetitions, as the center point moves downflow towards the last detection point, provides useful information for accurately declaring the source location. If the AUV starts the Reacquire behavior after crossing the plume without detecting, the repetitions of the Bowtie give the AUV several more chances to detect odor. If the AUV starts the Reacquire behavior across the flow from the plume, the repetitions of the Bowtie, at and upflow from the most upflow last detection point, will bring the AUV back towards the location where the plume is likely to be. The Bowtie is sufficiently wide so that it is able to recontact the plume as long as the plume has meandered across the flow less than 13 m away from the most upflow last detection point.

### 5.6 Declaration decision

The source declaration is not a separate behavior. Instead, it is a function that is called at the end of the Track-Out behavior. Each time that the Track-In ends, the last detection point is added to a list. That list is sorted according to distance along the direction of the flow. As long as the AUV is making progress up the plume, the first points on the list will be widely separated. When the AUV is near the source, the plume tracing maneuvers will cause several points on the list to be very near each other in the direction of the flow. When the first three points on the sorted list differ in the direction of the flow by less than 4 meters,

then the most upflow point on the list is declared as the source location. An additional error component is due to the fact that the vehicle navigation system may contain accumulated errors of approximately 10 m.

Note that the chemical source is on the bottom and that the AUV drives at a nonzero altitude above the bottom (altitude of 1.5 to 2.0 m is commanded). Therefore, the chemical plume does not rise to the altitude of the AUV, which is necessary for the AUV to detect the chemical, until the chemical has traveled some distance from the source in the direction of the flow. This distance is flow-dependent and is not known. Therefore, the declared source location is expected to have an error component, relative to the true source location, that is in the direction of the flow.

6. Field test results

Two variations of CPT algorithms were tested in four different sets of experiments. A first CPT algorithm, described with experimental results in (Farrell et al., 2003), was tested at San Clemente Island (SCI) CA in September 2002 and at SCI in November 2002. Based on the results of those tests, the Find, Reacquire, and Source Declaration behaviors were revised and the post-declaration maneuvers were added. The revised CPT strategy described herein using the parameters shown in Table 4 was experimentally tested at SCI in April 2003 and at Duck NC in June 2003 (Farrell et al., 2005). The April 2003 experiments successfully declared the source location on 7 of 8 experiments. The experiments included ground truth confirmation of declared source locations via sidescan sonar. The algorithms and field test results described herein, unless otherwise noted, are from the June 2003 experiments in Duck NC.

Symbol	Behavior	Value
$\lambda$	Find	5.0 s
$\beta$	Find	20 deg
$L_u$	Track_out	18.0 m
$L_c$	Track_out	18.0 m
$N_{re}$	Reacquire	2
K	Guidance	5.0
R	Guidance	10.0 m

Table 4. Parameter settings for CPT strategy for the April 2003 SCI and June 2003 Duck experiments.

Two types of missions were of interest during this set of experiments. The first mission type, labeled ST, contained a single chemical source in the OpArea. The ST mission was intended to find the plume, to trace a plume over a long distance, and to declare the source location. This mission demonstrates detection and tracing of plumes over long distances. The second mission type, labeled MT, may contain a few chemical sources in the OpArea. In an MT mission, the OpArea will be divided into subregions. The AUV will search each subregion for chemical until one of three events occurs. First, the search within a subregion may timeout. In this case, the subregions is declared source free and the AUV moves on to the next subregion. Second, the AUV may detect chemical and declare a source location within the region. It will then move on to the next subregion. Third, the AUV may trace chemical to the upflow edge of the region. In this case, a source will be declared at the intersection of the plume with the upper edge of the subregion and the AUV will move on to the next

subregion. When the declared source locations are analyzed at the end of an experiment it is up to the test director to decide whether source locations at the edge of a subregion are due to sources near that location or the result of plumes generated by sources in the adjacent region.

The AUV for these tests was the Albacore REMUS owned by SPAWAR in San Diego, CA. The REMUS was modified to contain a PC104 computer to run the AMP CPT algorithms. The AMP computer received sensor data from the REMUS computer via serial port, processed the sensor data, and output heading, speed, and depth/altitude commands to the REMUS computer via the same serial port. Up and down looking acoustic Doppler current profilers (ADCP) were onboard the REMUS. The AUV also had a CTD mounted onboard, but it was not used due to its slow response time. Also, the AUV used long baseline transducers with acoustic buoys in conjunction with dead-reckoning based on ADCP data to determine onboard AUV position. Finally, a fluorometer was mounted near the nose of the AUV. The fluorometer was capable of detecting Rhodamine dye from a source that was used to create the plume for these experiments. The fluorometer sample rate was 10 Hz.

Fig. 7 and Fig. 8 show the trajectory (solid line), chemical detection locations (x's), and declared source location (black dot) for two missions performed at Duck, NC in June of

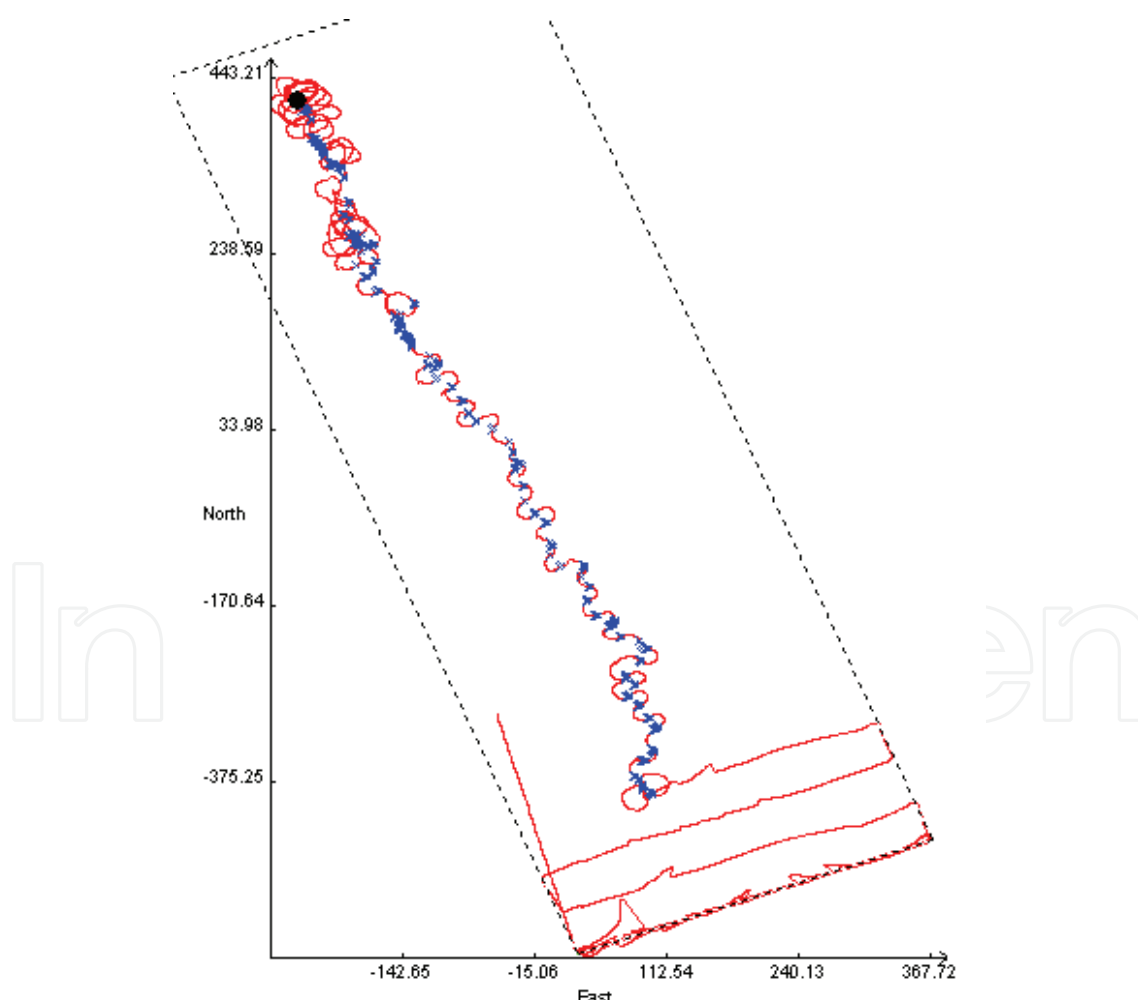


Fig. 7. Trajectory and chemical detection points. The dashed rectangle is the operating area boundary. The solid curve is the AUV trajectory. Each x marks the location of a chemical detection. The black dot at (N,E) = (414,-242)m marks the declared source location.



2003. The boundary of the OpArea is indicated by the dashed line. The figures use a coordinate system that is defined in the north and east directions relative to the center of the OpArea. These experiments were performed in 4-8 m of water. The bottom was gradually sloping from the coast. The coast is approximately 400 m to the left of boundary of the OpArea in both figures in this section. During all experiments included herein, the water column consisted of a top layer flowing northerly with a speed near 20-25 cm/s and a bottom layer flowing southerly with a speed near 10 cm/s. The depth of the boundary layer between these two flow regimes changed with location and time.

Fig. 7 shows the trajectory, chemical detection locations, and declared source location for an ST mission. For this mission, the OpArea was 367 x 1094 m (greater than 60 football fields). During this experiment, the flow calculated on the AMP varied in magnitude between 10 and 15 cm/s and in direction between 110 and 147 deg. For this experiment, the commanded speed was 2 m/s and the commanded altitude was 2 m. Note that the actual altitude varies by plus or minus 0.7 m relative to the commanded altitude. To challenge the CPT algorithm, we wanted the first chemical detection to occur as far as possible from the chemical source. Therefore, the source is located near the upflow edge of the OpArea and the AUV starts the mission near the downflow edge of the box. The AMP CPT algorithms start as soon as chemical is detected. This mission tracks the chemical plume for 976m between the first detection point and the declared source location. The source is declared at 36n11.028, 75w44.620. The ground truth source location is 36n11.035, 75w44.621 as found from sidescan data acquired during a post-declaration maneuver centered on the declared source location. The declared source location is 13 m south and 2 m east of the sidescan sonar location. Note that this error is predominantly in the direction of the flow, as expected. Fig. 8 shows the trajectory, chemical detection locations, and declared source locations for an MT mission. The four subregions are outlined by dashed lines in Fig. 8. During this experiment, the flow calculated on the AMP varied in magnitude between 20 and 30 cm/s and in direction between 160 and 175 degree. For this experiment, the commanded speed was 2 m/s and the commanded altitude was 1.5 m. The southwest region is explored first. Chemical is detected and tracked for 351 m to the boundary between the southwest and northwest regions. The source for the first region is declared (correctly) at this boundary. Then, AMP drives the AUV to the northwest region. In the northwest region, the plume is tracked for an additional 180 m with a source declared at 36n11.034, 75w44.621. Sidescan sonar data confirmed the source at 36n11.037, 75w44.622. The error between these locations is 6 m in the downflow direction. Note that this declared source is the same as that (for the same quadrant) from the missions shown in Fig. 7. Note that the latitude and longitude of the declared and sonar source locations match closely between these figures.

After declaring the source in the northwest region, AMP drove the AUV to the southeast region and restarted the CPT algorithm. During the transition from the northwest region to the southeast region using the Go To command, chemical detections are ignored. In the southwest region, chemical is detected and tracked a distance of 351 m to a source that is declared (correctly) on the boundary between the southeast and northeast regions. Then AMP drives the AUV to the northeast region. In the northeast region, the plume is tracked for an additional 185 m with the source declared at 36n11.079, 75w44.468. Sidescan sonar data confirmed the source at 36n11.087, 75w44.450. The error between these locations is 31 m in the crossflow direction. This crossflow error is clearly visible in the northeast region of Fig. 8. This crossflow error is an artifact of a navigation fix that occurred prior to the

declaration and the declaration logic that only accounted for position differences in the direction of the flow. This will be fixed in future versions of the algorithm.

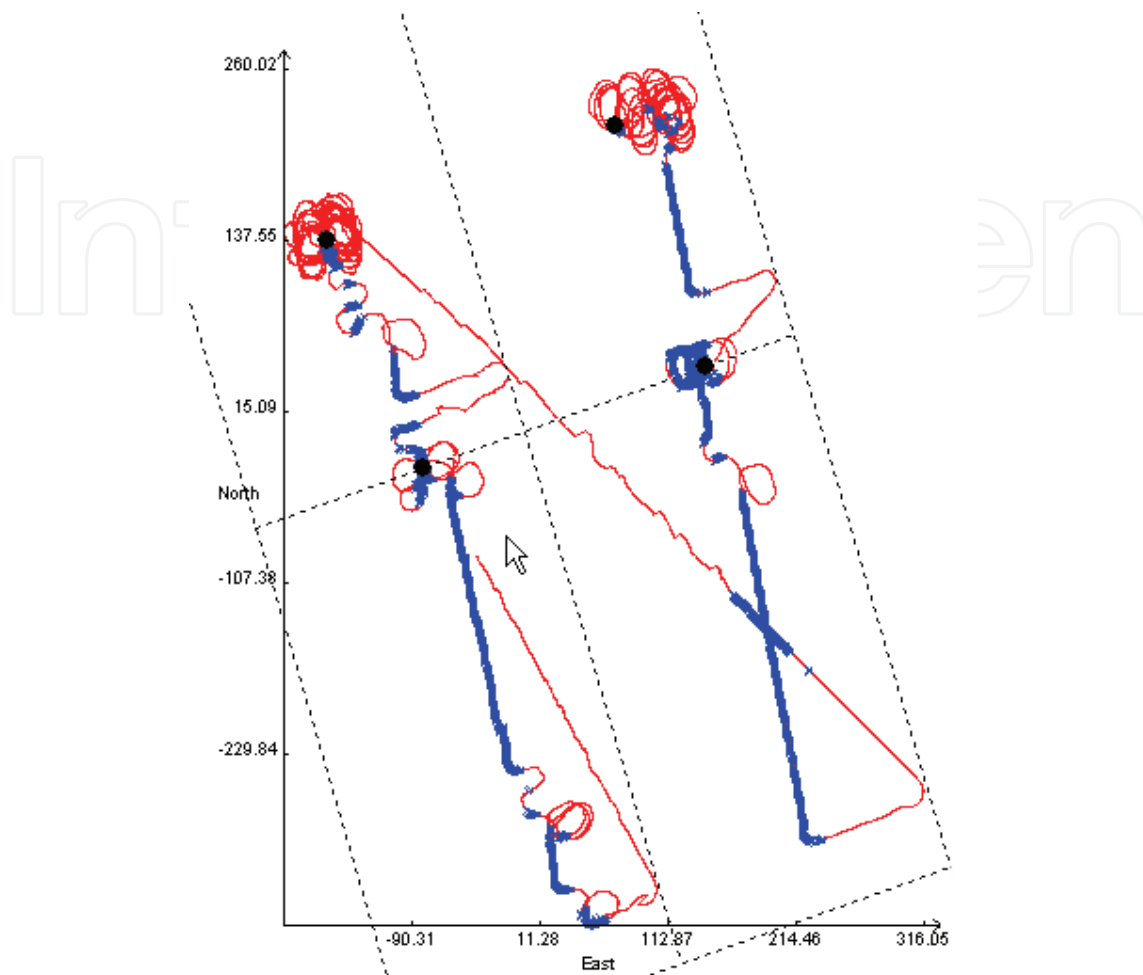


Fig. 8. Trajectory and chemical detection points. The dashed rectangle is the operating area. The solid curve is the AUV trajectory. Each x marks the location of a chemical detection. The black dots mark the declared source location.

Note that in spite of the exact same strategy and parameters being used in all runs, the nature of the trajectories shown in Fig. 7 and 8 during the plume tracing phase look different. Therefore, the differences in experimental conditions deserve comment. First, the mission shown in Fig. 7 was one of the first trials at Duck NC. Due to the fact that we were operating in an unknown environment, the commanded altitude for that mission was 2.0 m. For the mission corresponding to Fig. 8, the commanded altitude was 1.5 m. Analysis of the log files show that plume tracing for the mission of Fig. 7 frequently used the Track-Out behavior, which relies on large magnitude turns designed to cross the plume. Fig. 7 clearly shows this behavior. Plume tracing for the mission shown in Fig. 8 primarily used the Track-In behavior, since its small angle counterturning caused the AUV to drive up the main body of the plume. The difference in commanded altitudes could be the major reason for this difference, if the 2 m altitude of Fig. 7 only allowed the AUV to intermittently contact the top of the plume. Note also that in Fig. 8, as the AUV approaches the source, it must use the Track-Out behavior more frequently, because near the source the plume is still at a lower altitude.

The values of the parameters of the CPT strategy are summarized in Table 4. If  $\beta$  is increased, then the counterturns have a larger cross flow component. The tradeoff is that the larger crossflow component increases the probability that the AUV exits the plume from the expected edge (i.e., the variable LHS is more likely to be correct), but increases the length of the trajectory to get to the source. The variable  $\lambda$  should be larger than the intermittent chemical detection gaps while “in the plume;” however, the plume intermittency is dependent on characteristics of the flow and turbulence that are not known. Typical “in the plume” interpulse durations are less than 1s (Jones, 1983). As  $\lambda$  is increased, if chemical is not detected, then the distance that the AUV moves from the last detection point is increased. As long as this distance is less than  $L_u$ , then no backtracking is required. For these experiments,  $v_c = 2.0$  m/s. Therefore, for  $\lambda = 5$ s, the distance traveled is 10 m which is less than  $L_u$ . The value of  $L_c$  was selected to ensure that, even with navigation errors ( $<10$  m nominally) and with the Go To guidance command being satisfied when the AUV was within 10 m of the destination, the AUV would cross a line extending upflow from the last detection point. The value of  $N_{re}$  was set to 2. Increasing  $N_{re}$  causes the AUV to spend additional time searching upflow from each point on the *lost\_pnts* list. This additional time is detrimental when the BowTie’s are upflow from a false-alarm detection point. The values of  $K$  and  $R$  are dependent on the dynamic capabilities of the AUV. These values were determined in simulation and evaluated onboard the AUV prior to the CPT experiments described herein.

Note also, that the definition of a chemical detection implicitly contains two parameters: the detection threshold and the number of above threshold readings required to declare a detection. For all variations of CPT strategies that we performed during the three year program, the definition of a chemical detection was a concentration  $c(t) > 4\%$  of full scale (i.e., 0.2 V). This value was determined by analysis of chemical sensor data from the AUV operating in San Diego Bay (August 2002) in the absence of the chemical. In this scenario, the sensor readings were pure noise, but never surpassed 0.2 V. Therefore, we selected the threshold such that the probability of false alarm readings was extremely low. Therefore, any single sensor reading above threshold was registered as a chemical detection. The number of above threshold readings required to register a detection could be increased. This would decrease the probability of false alarms, but increase the probability of missed detections.

With the current AMP strategy and experimental results in mind, many alternative and possibly improved AMP strategies could be proposed. In fact, one of the goals of any experiment should be to identify areas for future improvements. Therefore, it is important to consider what lessons were learned in these experiments. First, care should be taken to ensure that the ADCP flow data corresponds to the flow layer containing the plume; however, this is not straightforward. For the Duck NC test location, the water is 4-8 m deep. The bottom boundary layer depth varied with time. The minimum safe AUV operating altitude was 1.5 m and the ADCP has an approximately 0.75 m deadzone prior to its measurement being accurate. Therefore, there were runs for which the upward looking ADCP was measuring the flow in the top layer instead of the bottom layer. Detecting and accommodating such events would require significant advancements for the planner and possibly a conductivity, temperature, and depth (CTD) sensor with a fast response time. Second, some of the declared source locations had unexpected error in the crossflow

direction, which was unexpected. We believe that this error component is due to navigation fixes that occurred near the time of declaration and by the declaration logic that ignored separation in the crossflow direction. The source declaration logic described herein was based only on the along flow separation of points at which the plume was lost. The crossflow separation was ignored in the declaration process to decrease the time required to make a declaration. Accounting for crossflow separation in the declaration logic would improve the accuracy of the declaration and is straightforward to implement in the future. Third, the current AMP strategy used the chemical sensor in a Boolean mode even though the sensor did provide an analog reading. It is often suggested that the analog concentration could provide a useful indicator of the distance to the source; however, there are a few difficulties in this approach. First, the chemical source concentration would be unknown in a real application. Second, the rate of decay of the peak concentration reading as a function of the distance from the source is flow dependent and not known. Third, maximum sensed concentration along any transect is not necessarily the maximum concentration in the vicinity of that transect. Alternative, the analog sensor reading could have utility in experiments where multiple sources might generate overlapping plumes. In that scenario, a significant decrease in the maximum sensed chemical while moving upflow might indicate that a source has just been passed by while the AUV is still in the plume of another source. Such strategies were not required for this project.

It is also interesting to consider adaptation of the AMP strategy parameters based on distance from the source. For example, it might be more efficient to decrease  $L_u$  and  $L_c$  as the AUV gets nearer to the source. The difficulty in implementing such ideas is in evaluating the distance to the source when the source location is unknown. Early in the program, we hoped that the width of plume transects would be a useful indicator of the distance to the source. This proved futile for a variety of reasons: plume meander results in AUV transects being at different angles relative to the plume centerline; a variety of factors result in AUV transects being at different altitudes relative to the plume centerline altitude; and, the instantaneous plume width at a fixed distance from the source varies widely. Similarly, sensed chemical concentration is not a useful indicator of distance to the source since the source concentration is unknown and the sensed concentration at a fixed distance from the source varies widely.

## 7. Conclusion

This chapter has presented adaptive mission planning algorithms and experimental results for the first demonstration of chemical signal guided AUV. The experiments occurred in a near shore ocean environment. Plume tracing was demonstrated over distances of 975 m with average source declaration accuracy of approximately 13 m. This error includes the unknown distance required for the plume to rise to the altitude at which the vehicle is traveling.

The CPT planning algorithms were developed based on behavior based planning techniques that the CPT problem was divided into several simple sub-problems (e.g., find problem, tracing problem, reacquiring problem). The find problem is to search a potentially large area to detect the plume for the first time; the tracing problem is to trace the plume to its source once the vehicle detects the chemical concentration over a threshold; the reacquiring

problem initiates a local search based on knowledge of the flow and past detection information to reacquire contact with the plume if contact with the plume is lost. At last, we developed the coordinating methodologies to switch between these strategies in an intelligent manner.

## 8. References

- Arbib, M. (1981). Perceptual Structures and Distributed Motor Control, In: *Handbook of Physiology - The Nervous Systems II*, Brooks (Ed.)
- Arkin, R. & Murphy, R. (1990). Autonomous navigation in a manufacturing environment, *IEEE Trans. Robot. Automation*, Vol. 6, 445-454.
- Basil, J. (1994). Lobster orientation in turbulent odor plumes: simultaneous measurements of tracking behavior and temporal odor patterns. *Biological Bulletin*, Vol. 187, 272-273
- Belanger, J. & Willis, M. (1998). Adaptive control of odor-guided location: Behavioral flexibility as an antidote to environmental unpredictability. *Adaptive Behavior*, Vol. 4, 217-253
- Bell, W. & Tobin T. (1982). Chemo-orientation. *Biol. Rev.*, Vol. 57, 219-260
- Berg, H. & A. Brown D. (1972). Chemotaxis in *Escherichia coli* analysed by three-dimensional tracking. *Nature*, Vol. 239, 500-504
- Berg, H. (1990). Bacterial microprocessing, In: *Cold Springs Harbor Symp. Quant. Biol.* 539-545
- Berg, H. (1993). *Random Walks in Biology*. Princeton University Press
- Berns, K.; Dillmann, R. & Hofstetter, R. (1991). An Application of a Backpropagation Network for the Control of a Tracking Behavior, *Proceedings of the IEEE International Conference on Robotics and Automation*, pp. 2426-2431
- Braitenberg, V. (1984). *Vehicles: Experiments in Synthetic Psychology*, MIT Press
- Brooks, R. (1986). A robust layered control system for a mobile robot, *IEEE Journal of Robotics and Automation*, Vol. 2, Num. 1, 14-23
- Cardé, R. & Mafra-Neto A. (1997). Insect Pheromone Research, In: *Mechanisms of flight of Male moths to pheromone*, pp. 275- 290. Chapman and Hall, New York
- Dubins, L. (1957). On Curves of Minimal Length with Constraint on Average Curvature, and with Prescribed Initial and Terminal Positions and Tangents. *American Journal of Mathematics*, Vol. 79, 497-516
- Dusenberry, D. (1992). *Sensory Ecology: How Organisms Acquire and Respond to Information*, W.H. Freeman, New York
- Elkinton, J.; Cardé, R & Mason, C. (1984). Evaluation of time-average dispersion models for estimating pheromone concentration in a deciduous forest. *Journal of Chemical Ecology*, Vol. 10, 1081-1108
- Farrell, J.; Li, W.; Pang, S. & Arrieta, R. (2003). Chemical Plume Tracing Experimental Results with a REMUS AUV. *MTS/IEEE Oceans 2003*
- Farrell, J.; Pang, S. & Li, W. (2005). Chemical Plume Tracing via an Autonomous Underwater Vehicle. *IEEE Journal of Ocean Engineering*, Vol. 30, Num. 2, 428-442
- Fossen, T. (1994). *Guidance and Control of Ocean Vehicles*. John Wiley & Sons
- Grasso, F.; Consi, T.; Mountain D. & Atema, J. (1996). Locating odor sources in turbulence with a lobster inspired robot, In: *From Animals to Animats 4: Proceedings of the Fourth*



- International Conference on Simulation of Adaptive Behavior*, P. Maes, M. J. Mataric, J.-A. Meyer, J. Pollack, and S. W. Wilson (Ed.), pp104-112, Cambridge, MA
- Grasso, F (2001). Invertebrate-inspired sensory-motor systems and autonomous, olfactory-guided exploration. *Biological Bulletin*, Vol. 200, 160-168
- Grasso, F.; Consi, T.; Mountain, D. & Atema, J. (2000). Biomimetic robot lobster performs chemo-orientation in turbulence using a pair of spatially separated sensors: Progress and challenges. *Robotics and Autonomous Systems*, Vol. 30, 115-131
- Hassler, A. & Scholz, A. (1983) *Olfactory Imprinting and Homing in Salmon* Springer-Verlag, New York
- Jones, C. (1983). On the structure of instantaneous plumes in the atmosphere. *Journal of Hazardous Materials*, Vol. 7, 87-112
- Li, W. ; Ma, C. & Wahl, F. (1997). A Neuro-Fuzzy System Architecture for Behavior-Based Control of a Mobile Robot in Unknown Environments, *Fuzzy Sets and Systems*, Vol. 87, 133-140
- Li, W.; Farrell, J. & R. T. Cardé (2001). Tracking of fluid-advected odor plumes: Strategies inspired by insect orientation to pheromone. *Adaptive Behavior*, Vol. 9, 143-170
- Li, W.; Farrell, J.; Pang, S. & Arrieta, R. (2006). Moth behavior based subsumption architecture for chemical plume tracing on a Remus autonomous underwater vehicle. *IEEE Transactions on Robotics and Automation*, Vol. 22, Num. 2, 292-307
- Lohmann, K. (1992). How sea turtles navigate. *Scientific America*, Vol. 266, 82-88
- Lytridis, C.; Kadar, E. & Virk, G. (2006). A systematic approach to the problem of odour source localisation. *Autonomous Robots*, Vol. 20, Num. 3, 261-276
- Martinez, D. (2007). Mathematical physics: On the right scent. *Nature*, Vol. 445, 371-372
- Murlis, J.; Elkinton, J. & Cardé, R (1992). Odor plumes and how insects use them. *Annual Review of Entomology*, Vol. 37, 505-532
- Mylne, K. (1992). Concentration fluctuation measurements in a plume dispersing in a stable surface layer. *Boundary-Layer Meteorology*, Vol. 60, 15-48
- Naeem W.; Sutton R.; Ahmad S. & Burns, R. (2003) A review of guidance laws applicable to unmanned underwater vehicles. *The Journal of Navigation*, Vol. 56, Num 1, 15-29
- Naeem W.; Sutton, R. & Chudley J. (2007). Chemical plume tracing and odour source localisation by autonomous vehicles. *Journal of Navigation*, Vol. 60, 173-190
- Nevitt, G. (2000). Olfactory foraging by antarctic procellariiform seabirds: Life at high Reynolds numbers. *Biol. Bull.*, Vol. 198, 245-253
- Shraiman, B. & Siggia, D. (2000). Scalar turbulence. *Nature*, Vol. 405, No. 8, 639-646
- Spears, D.; Zarzhitsky, D. & Thayer, D. (2005) Multi-robot chemical plume tracing. *Proceedings of the 2005 International Workshop on Multi-Robot Systems*, pp. 211-222
- Stacey, M.; Cowen, E.; Powell, T.; Dobbins, E.; Monismith, S. & Koseff J. (2000). Plume dispersion in a stratified, near-coastal flow: measurements and modeling, *Continental Shelf Research*, Vol. 20, 637--663
- Sutton, O. (1947). The problem of diffusion in the lower atmosphere. *Quart. J. Roy. Meteorol. Soc.*, Vol. 73, 257-281
- Sutton, O. (1953). *Micrometeorology*, McGraw-Hill, New York
- Vergassola, M.; Villermaux, E. & Boris I. Shraiman (2007). Infotaxis as a strategy for searching without gradients. *Nature*, Vol. 445, 406-409

- Vickers, N. (2000). Mechanisms of animal navigation in odor plumes. *Biological Bulletin*, Vol. 198, 203-212
- Wiesburg, M. & Zimmer-Faust R. (1994). Odor plumes and how blue crabs use them in finding prey. *J. Exp. Biol.*, Vol. 197, 349-375
- Zarzhitsky, D.; Spears, D.; Thayer, D. & Spears W. (2004). Agent-based chemical plume tracing using fluid dynamics. *Lecture Notes in Artificial Intelligence*, Vol. 3228 146-160
- Zimmer, R. & Butman, C. (2000). Chemical signaling processes in the marine environment: *Biological Bulletin*, Vol. 198, 168–187



## **Underwater Vehicles**

Edited by Alexander V. Inzartsev

ISBN 978-953-7619-49-7

Hard cover, 582 pages

**Publisher** InTech

**Published online** 01, January, 2009

**Published in print edition** January, 2009

For the latest twenty to thirty years, a significant number of AUVs has been created for the solving of wide spectrum of scientific and applied tasks of ocean development and research. For the short time period the AUVs have shown the efficiency at performance of complex search and inspection works and opened a number of new important applications. Initially the information about AUVs had mainly review-advertising character but now more attention is paid to practical achievements, problems and systems technologies. AUVs are losing their prototype status and have become a fully operational, reliable and effective tool and modern multi-purpose AUVs represent the new class of underwater robotic objects with inherent tasks and practical applications, particular features of technology, systems structure and functional properties.

### **How to reference**

In order to correctly reference this scholarly work, feel free to copy and paste the following:

Shuo Pang (2009). Chemical Signal Guided Autonomous Underwater Vehicle, Underwater Vehicles, Alexander V. Inzartsev (Ed.), ISBN: 978-953-7619-49-7, InTech, Available from:  
[http://www.intechopen.com/books/underwater\\_vehicles/chemical\\_signal\\_guided\\_autonomous\\_underwater\\_vehicle](http://www.intechopen.com/books/underwater_vehicles/chemical_signal_guided_autonomous_underwater_vehicle)

**INTECH**  
open science | open minds

### **InTech Europe**

University Campus STeP Ri  
Slavka Krautzeka 83/A  
51000 Rijeka, Croatia  
Phone: +385 (51) 770 447  
Fax: +385 (51) 686 166  
[www.intechopen.com](http://www.intechopen.com)

### **InTech China**

Unit 405, Office Block, Hotel Equatorial Shanghai  
No.65, Yan An Road (West), Shanghai, 200040, China  
中国上海市延安西路65号上海国际贵都大饭店办公楼405单元  
Phone: +86-21-62489820  
Fax: +86-21-62489821

© 2009 The Author(s). Licensee IntechOpen. This chapter is distributed under the terms of the [Creative Commons Attribution-NonCommercial-ShareAlike-3.0 License](https://creativecommons.org/licenses/by-nc-sa/3.0/), which permits use, distribution and reproduction for non-commercial purposes, provided the original is properly cited and derivative works building on this content are distributed under the same license.

IntechOpen

IntechOpen